ORGANIC CHEMISTRY
FRONTIERS

RESEARCH ARTICLE

View Article Online
View Journal | View Issue

CrossMark click for updates

Cite this: *Org. Chem. Front.*, 2014, **1**, 988

Received 30th June 2014,
Accepted 11th August 2014

DOI: 10.1039/c4qo00182f

rsc.li/frontiers-organic

Near-infrared absorbing heterocyclic quinoid donors for organic solar cell devices†‡

Emel Ay, Shunsuke Furukawa* and Eiichi Nakamura*

New heterocyclic quinoid donor molecules were designed and synthesized for application to organic solar cells in the near-infrared region. Devices using one of these quinoid molecules as a photoexcitable donor and C_{60} as an acceptor function in the visible and the near-infrared regions up to 890 nm.

Organic solar cells (OSCs) have attracted considerable attention in the past 30 years,[1] and academia-to-industry technology transfer has come to the stage of business development, such as building integrated applications that complement silicon solar cells.[2] The currently available OSCs only utilize visible light and, to further increase their efficiency, the development of organic materials that convert near-infrared (NIR) light into an electric current is essential.[3,4] Among various possible designs of narrow-band-gap materials for NIR absorption,[5] π-conjugated quinoidal molecules are promising candidates,[6] although they have intrinsic problems as OSC materials. First, they often show a biradical character because of the narrow band gap,[7] and are insufficiently stable for material applications. Second, stable quinoids usually have HOMO/LUMO levels that are too low to be practically useful because they contain electron-withdrawing groups to gain stability.[8] Here, we report the synthesis and properties of heterocyclic quinoid molecules **1–3** containing 4,5-diarylimidazol-2-ylidene units (Fig. 1), which are thermally stable and strongly absorb in the NIR region. The electron-rich quinoidal 2,5-dihydropyrroles **2** and **3** are capable of photoelectric conversion in the visible and the NIR regions up to 890 nm when used as a photoexcitable electron donor material in an OSC device where C_{60} is used as an electron acceptor. The central heterocyclic ring stabilizes the closed-shell quinoid form because of its low aromaticity, and hence is probably responsible for the high stability. The heteroatoms (*i.e.*, S and N) in the central rings donate an electron to the quinoidal system to raise the HOMO/LUMO levels.

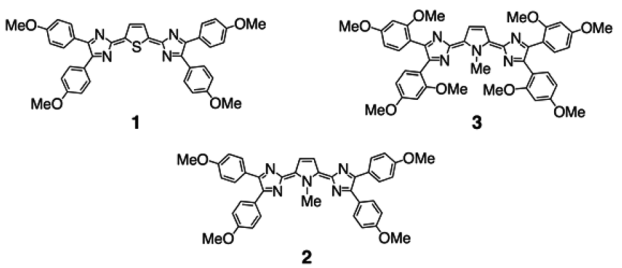

Fig. 1 Chemical structures of heterocyclic quinoid molecules **1–3**.

The synthesis of **1–3** was achieved using the Debus–Radziszewski reaction[9] with a heterole-2,5-dicarbaldehyde as the central building block and benzils as terminal blocks in the presence of ammonium acetate, followed by oxidation (Scheme 1). Reaction of thiophene-2,5-dicarbaldehyde (**4**) with 1,2-bis(4-methoxyphenyl)ethane-1,2-dione in the presence of ammonium acetate gave the cyclized product **5** in a moderate yield (62%). Treatment of **5** with an excess of potassium ferricyanide under basic conditions afforded the target quinoid compound **1** in a high yield (81%). Quinoid compounds **2** and **3** were also synthesized in a similar manner (synthetic details are given in ESI‡). Thermogravimetry–differential thermal analysis (TG–DTA) showed that the decomposition temperatures of the quinoid compounds are 264, 252, and 220 °C for **1**, **2**, and **3**, respectively, which are high enough for material application (Fig. S1 in ESI‡).

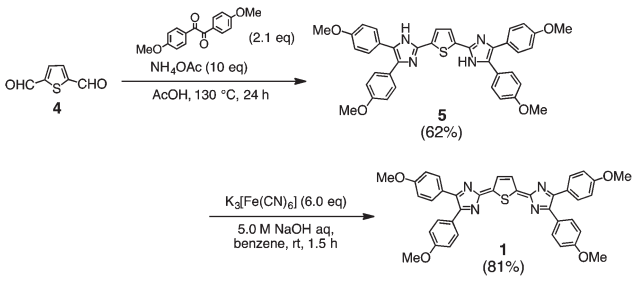

Scheme 1 Synthesis of the quinoid compound **1**.

Department of Chemistry, The University of Tokyo, Hongo, Bunkyo-ku, Tokyo, 113-0033, Japan. E-mail: f-shunsuke@chem.s.u-tokyo.ac.jp, nakamura@chem.s.u-tokyo.ac.jp; Fax: (+81) 3-5800-6889

† Dedicated to Professor Max Malacria on the occasion of his 65th birthday.

‡ Electronic supplementary information (ESI) available: Experimental details, compound characterization, TG-DTA data, CV data, PYS data and other materials. See DOI: 10.1039/c4qo00182f

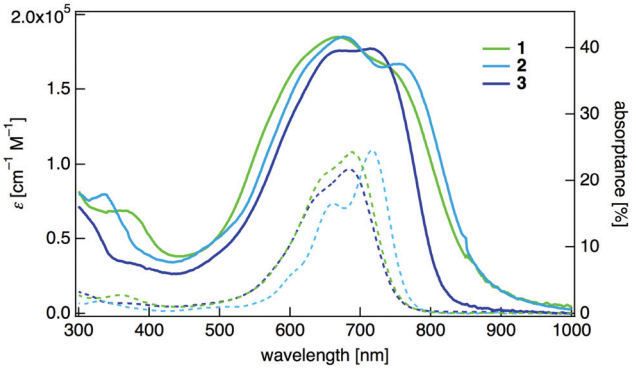

Fig. 2 UV-vis-NIR absorption spectra of **1–3** in CH_2Cl_2 (dashed lines) and absorption spectra of thin-film samples on a quartz substrate (solid lines).

The UV-vis-NIR absorption spectrum of the dihydrothiophene derivative **1** in dichloromethane showed an absorption maximum at 688 nm with a large molar absorption coefficient ($\log \varepsilon$ = 5.03) (Fig. 2, Table 1). The absorption spectrum of the dihydropyrrole **2** was red-shifted (λ_{max} = 716 nm, $\log \varepsilon$ = 5.04) compared with that of **1**. The 2,5-dimethoxyphenyl-substituted dihydropyrrole **3** showed a shorter wavelength absorption (λ_{max} = 684 nm, $\log \varepsilon$ = 4.99) than **2**, although the central π-system is of the same structure. This is probably because of larger dihedral angles between the 2,5-dimethoxyphenyl rings and the main quinoidal core in **3**. We also measured the absorptance spectra of thin films of these compounds, ensuring that light scattering and reflection effects were properly eliminated.[10] The absorptance spectra of all of these compounds were red-shifted (λ_{max} = 771 nm for **1**, λ_{max} = 784 nm for **2**, and λ_{max} = 744 nm for **3**) compared with the absorption spectra in CH_2Cl_2, and the broadened absorptions covered the entire visible spectral range and entered the NIR region.

The physical properties of the quinoid compounds suggest that these quinoid molecules are suitable as donor materials for OSC applications. The cyclic voltammograms (CVs) of **1** and **2** in dichloromethane showed a reversible oxidation wave at 0.66 V and 0.49 V (*vs.* Fc/Fc^+), respectively, and that of **3** showed two reversible oxidation waves at 0.44 V and 0.65 V (Fig. 2S in ESI‡). Thus, all of these quinoid molecules are stable for electrochemical oxidation. The estimated HOMO energy levels are −5.46, −5.29, and −5.24 eV for **1**, **2**, and **3**, respectively (Table 1). These compounds also showed two reversible reduction waves at −0.67 and −0.78 V for **1**, −0.85 and −1.01 V for **2**, and −0.92 and −1.11 V for **3**. The LUMO energy levels of **1**, **2**, and **3** were estimated to be −4.13, −3.95, and −3.88 eV, respectively. These LUMO energy levels are higher than those of representative quinoid molecules reported as n-type organic materials[6a,11] and would trigger the photoinduced electron transfer from these molecules to acceptor molecules. We also investigated the energy levels of **1–3** in thin films. The ionization potentials (IPs) obtained by photoelectron yield spectroscopic (PYS) measurements for a thin film were 4.90, 4.81, and 4.70 eV for **1**, **2**, and **3**, respectively, which are higher by as much as 0.56 eV than E_{HOMO} determined in solution (*vide supra*). Similarly, the electron affinities (EAs) estimated for the film samples are higher than those for solutions. Intermolecular interactions are known to affect greatly the HOMO/LUMO energy levels of quinoid molecules in the solid state.[12]

We fabricated OSC devices using **1–3** as a donor material and C_{60} as an acceptor: ITO/PEDOT:PSS/quinoid donor/C_{60}/NBphen/Al, where PEDOT:PSS, C_{60}, and NBphen serve as an anode buffer, an acceptor, and a cathode buffer, respectively (Fig. 3(a)). For device **A**, 2,5-dihydrothiophene **1** was spin-coated on the anode buffer. For devices **B** and **C**, 2,5-dihydropyrroles **2** and **3**, respectively, were used as a donor layer (see ESI‡ for details). The OSC performance was examined under irradiation with 100 mW cm^{-2} incident light using an AM 1.5G filter.

Devices **B** and **C** using electron-rich donors **2** and **3** showed much better performance than **A** using **1**. The current density (J)–voltage (V) dependence of device **A** using **1** showed a very low power conversion efficiency (PCE) of 0.02% with an open-circuit voltage (V_{oc}) of 0.49 V, a short-circuit current density (J_{sc}) of 0.23 mA cm^{-2}, and a fill factor (FF) of 0.19 (Fig. 3(b), Table 2). The plot of incident photon-to-current efficiency (IPCE) *vs.* wavelength of device **A** indicated that photocurrent conversion does not take place in the NIR region in spite of absorption by donor **1** up to 950 nm (Fig. 3c).

In the light of the EA of **1** (3.58 eV) and that of C_{60} (3.98 eV),[13] we consider that the band offset of these two states is too small to generate free mobile charges at the donor/acceptor interface,[14] resulting in the small J_{sc} and IPCE (Table 2). In contrast, devices **B** and **C** using the electron-rich 2,5-dihydropyrroles **2** and **3** showed much higher J_{sc} values of 1.64 mA cm^{-2} for device **B** and 2.34 mA cm^{-2} for device **C**. Other parameters for devices **B** and **C** are also shown in Table 2. The IPCE spectra of these devices indicate that **2** and **3** effect photocurrent generation at 890 and 850 nm for devices

Table 1 Photoelectronic properties of the quinoid molecules **1–3**

	λ_{max} [nm] in CH_2Cl_2 ($\log \varepsilon$)	λ_{max} [a] [film, nm]	E_{HOMO} [b] [solution, eV]	E_{LUMO} [c] [solution, eV]	IP[d] [film, eV]	EA[e] [eV]
1	688 (5.03)	667, 771	−5.46	−4.13	4.90	3.58
2	716 (5.04)	673, 784	−5.29	−3.95	4.81	3.39
3	684 (4.99)	659, 744	−5.24	−3.88	4.70	3.32

[a] Absorption maxima λ_{max} determined by curve fitting to the experimental spectra with multi-Gaussian peaks. [b] HOMO energy levels estimated from CV measurements in CH_2Cl_2. [c] LUMO energy levels estimated from CV measurements in CH_2Cl_2. [d] IPs of the thin films determined by PYS. [e] EAs estimated from the following equation: EA = IP − E_g, where E_g refers to the optical energy gap calculated using $1240/\lambda_{onset}$.

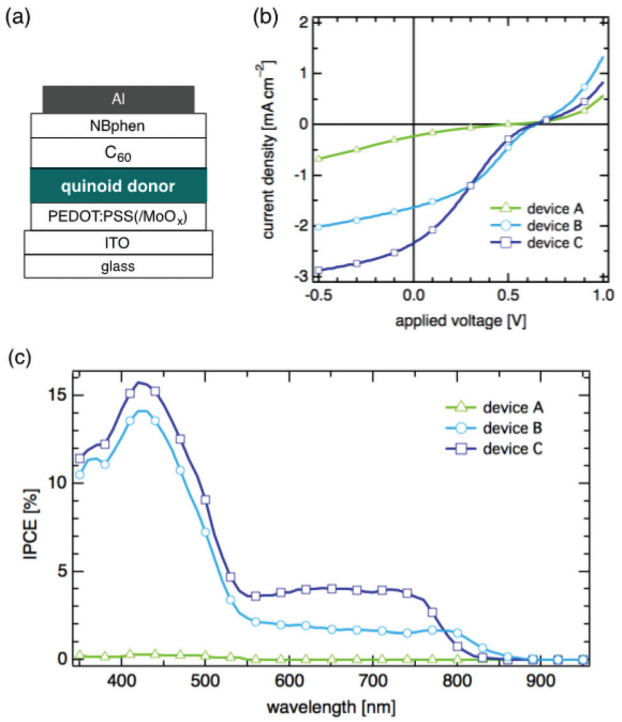

Fig. 3 The configuration of the fabricated OSC devices **A**, **B**, and **C** using the quinoid materials **1**, **2**, and **3**, respectively, as a donor layer (a), *J*–*V* characteristics (b) and IPCE profiles (c) of the devices. For devices **B** and **C**, a molybdenum oxide (MoO_x) layer was inserted between the PEDOT:PSS and the quinoid donor layers.

Table 2 Summary of the photovoltaic characteristics of devices **A**–**C** involving the quinoid compounds as a donor layer

	Donor	V_{oc} [V]	J_{sc} [mA cm^{-2}]	FF	PCE [%]
Device **A**	**1**	0.49	0.23	0.19	0.02
Device **B**	**2**	0.65	1.64	0.35	0.37
Device **C**	**3**	0.63	2.34	0.25	0.37

B and **C**, respectively. In view of the higher IPCE of device **C** than that of device **B**, we may speculate that the higher EA of quinoid **3** enhances the generation of free mobile charges at the donor/acceptor interface.

In summary, we have designed new NIR-absorbing quinoid dyes **1**–**3** for OSCs through the combination of a central heterocyclic ring and electron-donating terminal substituents. The three new quinoid compounds are thermally stable, absorb strongly in the NIR range, and have HOMO/LUMO levels suitable for OSC applications. OSC devices using **2** and **3** indeed function both in the visible and in the NIR ranges.

Acknowledgements

S. F. thanks MEXT for KAKENHI no. 26870144, and E. N. thanks the Strategic Promotion of Innovation Research and Development from the Japan Science and Technology Agency (JST).

Notes and references

1 (*a*) *Organic Photovoltaics: Concepts and Realization*, ed. C. Brabec, V. Dyakonov, J. Parisi and N. S. Sariciftci, Springer-Verlag, Berlin, 2003; (*b*) F. C. Krebs, *Sol. Energy Mater. Sol. Cells*, 2009, **93**, 394.

2 (*a*) R. F. Service, *Science*, 2011, **332**, 293; (*b*) M. C. Scharber and N. S. Sariciftci, *Prog. Polym. Sci.*, 2013, **38**, 1929; (*c*) Y. Matsuo, Y. Sato, T. Niinomi, I. Soga, H. Tanaka and E. Nakamura, *J. Am. Chem. Soc.*, 2009, **131**, 16048; (*d*) H. Tsuji, K. Sato, Y. Sato and E. Nakamura, *Chem. – Asian J.*, 2010, **5**, 1294; (*e*) H. Tsuji, Y. Yokoi, Y. Sato, H. Tanaka and E. Nakamura, *Chem. – Asian J.*, 2011, **6**, 2005; (*f*) H. Tsuji, Y. Ota, S. Furukawa, C. Mitsui, Y. Sato and E. Nakamura, *Asian J. Org. Chem.*, 2012, **1**, 34; (*g*) H. Tanaka, Y. Abe, Y. Matsuo, J. Kawai, I. Soga, Y. Sato and E. Nakamura, *Adv. Mater.*, 2012, **24**, 3521; (*h*) K. Harano, S. Okada, S. Furukawa, H. Tanaka and E. Nakamura, *J. Polym. Sci., Part B: Polym. Phys.*, 2014, **52**, 833.

3 (*a*) M. C. Scharber, D. Mühlbacher, M. Koppe, P. Denk, C. Waldauf, A. J. Heeger and C. J. Brabec, *Adv. Mater.*, 2006, **18**, 789; (*b*) G. Nennler, M. C. Scharber, T. Ameri, P. Denk, K. Forberich, C. Waldauf and C. J. Brabec, *Adv. Mater.*, 2008, **20**, 579.

4 (*a*) E. Bundgaard and F. C. Krebs, *Sol. Energy Mater. Sol. Cells*, 2007, **91**, 954; (*b*) R. Kroon, M. Lenes, J. C. Hummelen, P. W. M. Blom and B. de Boer, *Polym. Rev.*, 2008, **48**, 531.

5 (*a*) G. Qian and Z. Y. Wang, *Chem. – Asian J.*, 2010, **5**, 1006; (*b*) J. Fabian, H. Nakazumi and M. Matsuoka, *Chem. Rev.*, 1992, **92**, 1197.

6 (*a*) T. Takahashi, K. Matsuoka, K. Takimiya, T. Otsubo and Y. Aso, *J. Am. Chem. Soc.*, 2005, **127**, 8928; (*b*) K. Zhang, K.-W. Huang, J. Li, J. Luo, C. Chi and J. Wu, *Org. Lett.*, 2009, **11**, 4854; (*c*) X. Zhu, H. Tsuji, K. Nakabayashi, S. Ohkoshi and E. Nakamura, *J. Am. Chem. Soc.*, 2011, **133**, 16342.

7 (*a*) Z. Zeng, Y. M. Sung, N. Bao, D. Tan, R. Lee, J. L. Zafra, B. S. Lee, M. Ishida, J. Ding, J. T. L. Navarrete, Y. Li, W. Zeng, D. Kim, K.-W. Huang, R. D. Webster, J. Casado and J. Wu, *J. Am. Chem. Soc.*, 2012, **134**, 14513; (*b*) A. Shimizu, T. Kubo, M. Uruichi, K. Yakushi, M. Nakano, D. Shiomi, K. Sato, T. Takui, Y. Hirao, K. Matsumoto, H. Kurata, Y. Morita and K. Nakasuji, *J. Am. Chem. Soc.*, 2010, **132**, 14421; (*c*) T. Kubo, A. Shimizu, M. Sakamoto, K. Uruichi, K. Yakushi, M. Nakano, D. Shiomi, K. Sato, T. Takui, Y. Morita and K. Nakasuji, *Angew. Chem., Int. Ed.*, 2005, **44**, 6564; (*d*) M. Kozaki, A. Isoyam and K. Okada, *Tetrahedron Lett.*, 2006, **47**, 5375.

8 (*a*) J. Casado, R. P. Ortiz and J. T. López Navarrete, *Chem. Soc. Rev.*, 2012, **41**, 5672; (*b*) M. Kozaki, A. Isoyama, K. Akita and K. Okada, *Org. Lett.*, 2005, **7**, 115; (*c*) Y. Suzuki,

M. Shimawaki, E. Miyazaki, I. Osaka and K. Takimiya, *Chem. Mater.*, 2011, **23**, 795; (*d*) J. Casado, M. Z. Zgierski, P. C. Ewbank, M. W. Burand, D. E. Janzen, K. R. Mann, T. M. Pappenfus, A. Berlin, E. Pérez-Inestrosa, R. P. Ortiz and J. T. López Navarrete, *J. Am. Chem. Soc.*, 2006, **128**, 10134.

9 Z. Wang, in *Comprehensive Organic Name Reactions and Reagents*, John Wiley & Sons, Inc., 2009, p. 2293; and references therein.

10 The absorbance (%*A*) was calculated using the following equation: %*A* = 100 − (%*T* + %*R*), where %*T* is transmittance and %*R* is reflectance of the thin films.

11 (*a*) T. M. Pappenfus, B. J. Hermanson, T. J. Helland, G. G. W. Lee, S. M. Drew, K. R. Mann, K. A. McGee and S. C. Rasmussen, *Org. Lett.*, 2008, **10**, 1553; (*b*) Q. Wu, R. Li, W. Hong, H. Li, X. Gao and D. Zhu, *Chem. Mater.*, 2011, **23**, 3138; (*c*) Y. Suzuki, E. Miyazaki and K. Takimiya, *J. Am. Chem. Soc.*, 2010, **132**, 10453.

12 J. C. Ribierre, S. Watanabe, M. Matsumoto, T. Muto, A. Nakao and T. Aoyama, *Adv. Mater.*, 2010, **22**, 4044.

13 H. Yoshida, *MRS Symp. Proc.*, 2013, **1493**, 295.

14 (*a*) A. A. Bakulin, A. Rao, V. G. Pavelyev, P. H. M. van Loosdrecht, M. S. Pshenichnikov, D. Niedzialek, J. Comil, D. Beljonne and R. H. Friend, *Science*, 2012, **335**, 1340; (*b*) A. E. Jailaubekov, A. P. Willard, J. R. Tritsch, W.-L. Chan, N. Sai, R. Gearba, L. G. Kaake, K. J. Williams, K. Leung, P. J. Rossky and X.-Y. Zhu, *Nat. Mater.*, 2013, **12**, 66.